Supplementary materials to

"A new geological slip rate estimate for the Calico Fault, eastern California: Implications for geodetic versus geologic rate estimates in the Eastern California Shear Zone"

Surui Xie[a], Elisabeth Gallant[a], Paul H. Wetmore[a], Paula M. Figueiredo[b], Lewis A. Owen[b], Craig Rasmussen[c], Rocco Malservisi[a], Timothy H. Dixon[a]

a. School of Geosciences, University of South Florida, Tampa, FL, USA

b. Department of Geology, University of Cincinnati, Cincinnati, OH, USA

c. Department of Soil, Water and Environmental Science, University of Arizona, Tucson, AZ, USA

Correspondence: Surui Xie <suruixie@mail.usf.edu>

Contents:

S1. Optically stimulated luminescence dating

S1.1 Preparation and measurement

Three OSL samples were collected at 75, 55 and 33 cm of depth (Calico F1, Calico F2 and Calico F3 respectively) by hammering 15-cm-long, 5-cm diameter plastic tubes into the sediment (Figure S7). The tubes remain sealed until opened and processed in the Luminescence Dating Laboratory at the University of Cincinnati under safe light conditions. A 2.5-cm-thick layer of sediment was removed from each end of each tube to obtain sediment from the center of the tube for processing and to reduce the possibility of that any sampled sediment was exposed to daylight since sampling. The sediment from the ends of each of the tubes was dried to determine the water content for each sample. The sediment was then crushed and sent to the Activation Laboratories Limited in Ancaster, Ontario, Canada for Major Elements Fusion ICP/MS/Trace Elements analysis to determine the U,Th and K concentrations for D_R calculations (Table 1 in the main article).

The remaining sediment was pretreated with 10% HCl and 10% H_2O_2 to remove carbonates and organic matter, respectively. The pretreated samples were rinsed in water, dried and sieved to recover the 90–155 μm particle size fraction. A sub-fraction (~20 g) of sample was etched using 44% HF acid for 80 minutes to remove the outer alpha irradiated layer from quartz particles. This treatment also helps dissolves any feldspars present. Any fluorides precipitated during HF treatment were removed using concentrated HCl for 30 min. The quartz sample was then rinsed in distilled water and acetate, and dried and sieved to obtain grain size 90–155 μm in diameter. Next, a low-field controlled Frantz isodynamic magnetic separator (LFC Model-2)

was used to separate feldspar and magnetic minerals from quartz in the 90–155 μm particle size fraction following the methods of Porat (2006) with the forward and side slopes set at 100° and 10°, respectively, within a variable magnetic field. The quartz was sieved using a 90 μm mesh to remove any grains smaller than 90 μm, so that the 90–155 μm could be used for OSL measurement.

An automated Riso OSL reader model TL-DA-20 was used for OSL measurements and irradiation. Aliquots, containing approximately several hundred grains of the samples, were mounted onto ~6 mm-diameter stainless steel discs as a small central circle ~3 mm in diameter. Aliquots for each sample were first checked for feldspar contamination using infrared stimulated luminescence (IRSL) at room temperature before the main OSL measurements were undertaken (Jain and Singhvi, 2001; Figure S8). If the aliquots did not pass the IRSL test the samples were etched in 40% HF for further 30 minutes to remove any feldspar, followed by 10% HCl treatment and sieving again. Samples that passed the IRSL test were used for OSL dating. Aliquots of samples were illuminated with blue LEDs stimulating at a wavelength of 470 nm (blue light stimulated luminescence – BLSL). The detection optics comprised Hoya U-340 and Schott BG-39 color glass filters coupled to an EMI 9235 QA photomultiplier tube. The samples were irradiated using a $^{90}Sr/^{90}Y$ beta source. The single aliquot regeneration (SAR) method of (Murray and Wintle, 2000, 2003) was used to determine the D_E for age estimation. Only aliquots that satisfy the criterion of a recycling ratio not more than 10% were used in determining D_E. A preheat of 240 ˚C for 10s was used and the OSL signal was recorded for 40s at 125˚C. OSL sensitivity of the samples had a high signal to noise

ratio. Dose recovery tests (Wintle and Murray, 2006) indicate that a laboratory dose of 10.9 Gy could be recovered to within 10% by the SAR protocol suggesting that the protocol was appropriate.

The natural OSL signals for all aliquots were at least an order of magnitude greater than background signal (Figure S8). The shine down curves (luminescence stimulated in the lab over 40s of exposure to light) for all aliquots showed fast decay patterns that confirm that the signal is the fast component of luminescence, which is dominant in quartz. This provides confidence that the sample would likely have been bleached quickly if only briefly exposed to sunlight. IRSL 'shine down' curves were used to test that there was no feldspar within the sample. Dose rate recovery tests for the samples shows that they have good recovery within the uncertainty of the laboratory measurement. Most aliquots provided good recuperation (<10%) and adequate recovery. The dose rate recovery was good for all samples (within 5% of assigned dose), which provides confidence in the suitability of the sediment for OSL dating. The spread of D_E was relatively large for some samples (Calico F2 and Calico F3; Figure S9 and Table 1 in the main article), which suggests possible partial bleaching. This can result in an overestimate of the age. We therefore separate the population of D_E values using a two-mixing model when the dispersion of D_E values was >20% and calculate the age of the lowest value population of D_E values (minimum peak in Figure S9; Table 1 in the main article).

S2. Terrestrial cosmogenic nuclide ^{10}Be dating

S2.1 Rock samples

We collected rock samples rich in quartz (>150 g each) from the upper 2 to 10 cm of the surface of large boulders, if available. Otherwise, whole cobbles were collected. Figure S1 shows the typical surface of the ALR alluvial fan. Figure S10 shows pictures for each sample used for TCN dating.

Samples were prepared at the University of Cincinnati using standard processing procedures, following *Gray et al.* (2014), *Frankel et al.* (2015), and *Hedrick et al.* (2017), and summarized here. Major steps included

1) Rock crushing: samples were crushed and sieved to obtain 0.25–0.5 mm grains;

2) Magnetic separation: we used currents of 0.4, 0.7, 1.0, and 1.4 amperes to separate out non-magnetic fractions for further processing;

3) Acid leaches: aqua regia with a mixture of 10% HCl/HNO_3 for 12–24 h followed by at least one 5% HF/HNO_3 and 1% HF/HNO_3 leaches each during ~24 h;

4) Mineral separation (if necessary): if heavy minerals were present that could not be removed by acids, LST (lithium heteropolytungstate) heavy liquid separation was applied; in addition LST also separates silicates with lower density than quartz, like feldspar. Samples with little quartz left (typically less than 5 grams) were not processed;

5) Dissolution and chemical purification: atomic absorption spectrometry Be carrier was added to the purified quartz, dissolved in concentrated HF, and passed through anion and cation exchange columns to extract $Be(OH)_2$. Blank samples were introduced at this stage and went through the same processing procedures following this step;

6) Calcination and target loading: $Be(OH)_2$ was calcinated in a furnace at 800 °C, then mixed

with niobium powder and loaded in steel targets.

Targets were measured with accelerator mass spectrometry (AMS), using the facility at the Purdue Rare Isotope Measurement Laboratory (PRIME Lab).

Rock sample ages were calculated using the online CREp program (crep.crpg.cnrs-nancy.fr) (*Martin et al.*, 2017). No shielding correction was need since there was no high-relief landforms around the study area. Rock density was set to be 2.7 g/cm^3. We assumed zero erosion on the surface. Other settings can be found in the footnotes of Table S1.

S2.2 Depth profiles

Alluvial fan surfaces at locations are representative of the characteristics of the ALR and TR alluvial fans. We dug trenches at these three locations to ~2 m depth. The two depth profiles in the ALR alluvial fan are named CalicoA and Calico-Pit3, and the profile in the TR alluvial fan is named Calico-Pit2. Approximately 1 kg of sediment was collected for each sample depths in the profiles, typically mixed of sand and pebbles. We sieved the sediment on site to obtain the < 2 cm fraction.

Sediment samples were processed with the same procedures as rock samples, except for the rock crushing step. Instead, we sieved each sediment sample directly in the laboratory to obtain the 0.25–0.5 mm fraction for ^{10}Be dating. However, samples from Calico-Pit2 and

Calico-Pit3 had little amount of quartz, so we crushed small pebbles with sizes 0.5–12.5 mm and included them in subsequent processing.

For CalicoA and Calico-Pit3, surface exposure ages were calculated using *Hidy*'s (2013) MATLAB-based Bayesian-Monte Carlo simulator. We set the reference production rate of 4.21±0.13 atoms/g/yr (same as the Western USA region in the CREp calculator). We used the time-dependent scaling scheme of *Stone* (2000) and a shielding value of 1.0, identical to the rock samples. Density was assumed to be a stochastic uniform distribution between 1.9 and 2.5 cm^3. For CalicoA, due to the data scatter, confidence level of 5σ was necessary to run the simulator (similarly as Hedrick et al. (2017)).

References

Balco, G., Stone, J. O., Lifton, N. A., and Dunai, T. J. (2008), A complete and easily accessible means of calculating surface exposure ages or erosion rates from 10 Be and 26 Al measurements. Quaternary geochronology, 3(3), 174-195.

Borchers, B., Marrero, S., Balco, G., Caffee, M., Goehring, B., Lifton, N., Nishiizumi, K., Phillips, F., Schaefer, J. and Stone, J. (2016), Geological calibration of spallation production rates in the CRONUS-Earth project. Quaternary Geochronology, 31, 188-198.

Frankel, K.L., Owen, L.A., Dolan, J.F., Knott, J.R., Lifton, Z.M., Finkel, R.C. and Wasklewicz, T., (2015), Timing and rates of Holocene normal faulting along the Black Mountains fault zone, Death Valley, USA. Lithosphere, 8(1), 3-22.

Gray, H. J., Owen, L. A., Dietsch, C., Beck, R. A., Caffee, M. A., Finkel, R. C., and Mahan, S. A. (2014), Quaternary landscape development, alluvial fan chronology and erosion of the Mecca Hills at the southern end of the San Andreas fault zone. Quaternary Science Reviews, 105, 66-85.

Hedrick, K.A., Owen, L.A., Chen, J., Robinson, A., Yuan, Z., Yang, X., Imrecke, D.B., Li, W., Caffee, M.W., Schoenbohm, L.M. and Zhang, B., 2017, Quaternary history and landscape evolution of a high-altitude intermountain basin at the western end of the Himalayan-Tibetan orogen, Waqia Valley, Chinese Pamir. Geomorphology. v. 284, p. 156-174. doi: 10.1016/ j.geomorph.2016.09.002

Hidy, A. (2013), Cosmogenic Nuclide Quantification of Paleo-fluvial Sedimentation Rates in Response to Climate Change. Ph.D Thesis, Dalhousie University, Halifax.

Jain, M., and Singhvi, A.K., 2001, Limits to depletion of blue-green light stimulated luminescence in feldspars: implications for quartz dating. Radiation Measurements, v. 33(6), p.883-892. doi:10.1016/S1350-4487(01)00104-4

Lal, D. (1991), Cosmic ray labeling of erosion surfaces: in situ nuclide production rates and erosion models. Earth and Planetary Science Letters, 104(2-4), 424-439.

Martin, L.C.P., Blard, P.-H., Balco, G., Lavé, J., Delunel, R., Lifton, N., and Laurent, V. (2017) The CREp program and the ICE-D production rate calibration database: A fully parameterizable and updated online tool to compute cosmic-ray exposure ages, Quaternary Geochronology, doi: 10.1016/j.quageo.2016.11.006.

Murray, A.S., and Wintle, A.G., 2000, Luminescence dating of quartz using an improved single-aliquot regenerative-dose protocol. Radiation Measurements v. 32(1), p. 57-73. doi: 10.1016/S1350-4487(99)00253-X

Murray, A.S., and Wintle, A.G., 2003, The single aliquot regenerative dose protocol: potential for improvements in reliability. Radiation Measurements, v. 37(4-5): p. 377-381. doi: 10.1016/S1350-4487(03)00053-2

Muscheler, R., Beer, J., Kubik, P.W. and Synal, H.A. (2005), Geomagnetic field intensity during the last 60,000 years based on 10 Be and 36 Cl from the Summit ice cores and 14 C. Quaternary Science Reviews, *24*(16), 1849-1860.

Nishiizumi, K., Winterer, E. L., Kohl, C. P., Klein, J., Middleton, R., Lal, D., and Arnold, J. R. (1989), Cosmic ray production rates of 10Be and 26Al in quartz from glacially polished rocks. Journal of Geophysical Research: Solid Earth, 94(B12), 17907-17915.

Porat, N., 2006, Use of magnetic separation for purifying quartz for luminescence dating. Ancient TL, v. 24(2), p.33-36.

Stone, J. O. (2000), Air pressure and cosmogenic isotope production. Journal of Geophysical Research: Solid Earth, 105(B10), 23753-23759.

Valet, J.P., Meynadier, L. and Guyodo, Y. (2005), Geomagnetic dipole strength and reversal rate over the past two million years. Nature, *435*(7043), 802-805.

Wintle, A.G., and Murray, A.S., 2006, A review of quartz optically stimulated luminescence characteristics and their relevance in single-aliquot regeneration dating protocols. Radiation Measurements, v. 41(4), p. 369-391. doi:10.1016/j.radmeas.2005.11.001

Figure S1. Typical surface of the ALR alluvial fan. Dark varnished pebbles and boulders on well developed desert pavement.

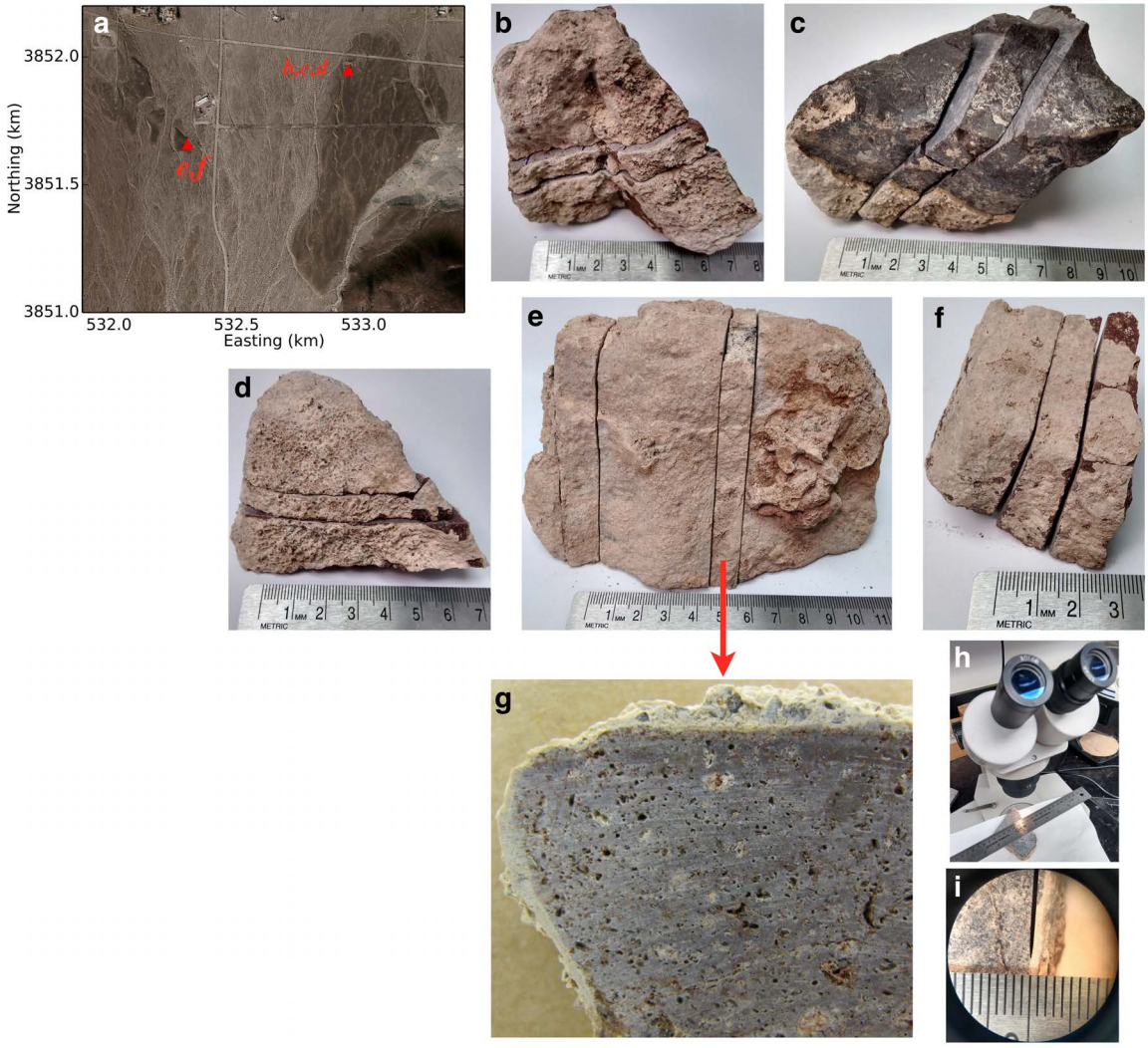

Figure S2. Carbonate rind thickness measurements for the ALR fan. (a) Red triangles mark locations of samples. b, c, and d correspond to samples shown in (b-d), they are exposed rocks collected at a scarp; e and f are two samples collected from the depth profile of Calico-Pit3, shown in (e) and (f). (b-f) Samples used to measure carbonate rind thickness, cut by a slow speed saw. (g) shows a cross-section of (e). (h) shows a sample under a ×10 binocular scope. (i) shows a measurement scene. Note that adjacent measurements are separated by ~2 cm.

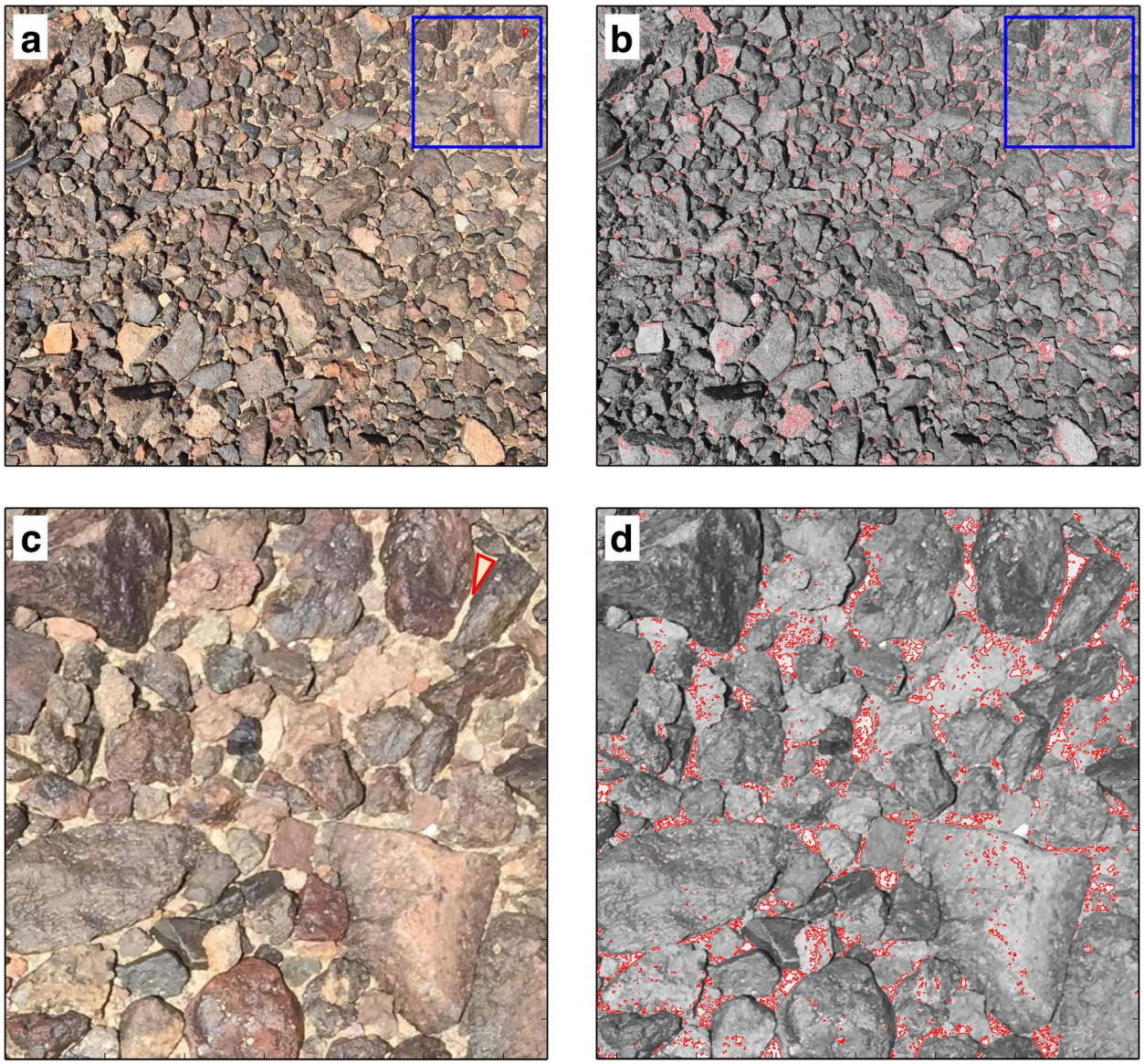

Figure S3. Estimate of pebble coverage percentage for the ALR fan surface. (a) is a nature color photo taken at approximately local noon, blue box mark the area shown in (c) and (d), red shape outlines an area of sand used as reference to detect mantle or sand coverage. We use the mean red/green/blue values and their 2 standard derivations of all pixels within the red shape to estimate surface areas that are covered by sand, hence percentage of pebble coverage. Red contours in grey color image (b) mark areas determined as sand. Percentage of pebble coverage at this site is 97%. Note this is an underestimate of pebble coverage due to the loose constraints we applied to determine sand coverage. Figure S4-S6 are three other sample areas with the same method applied.

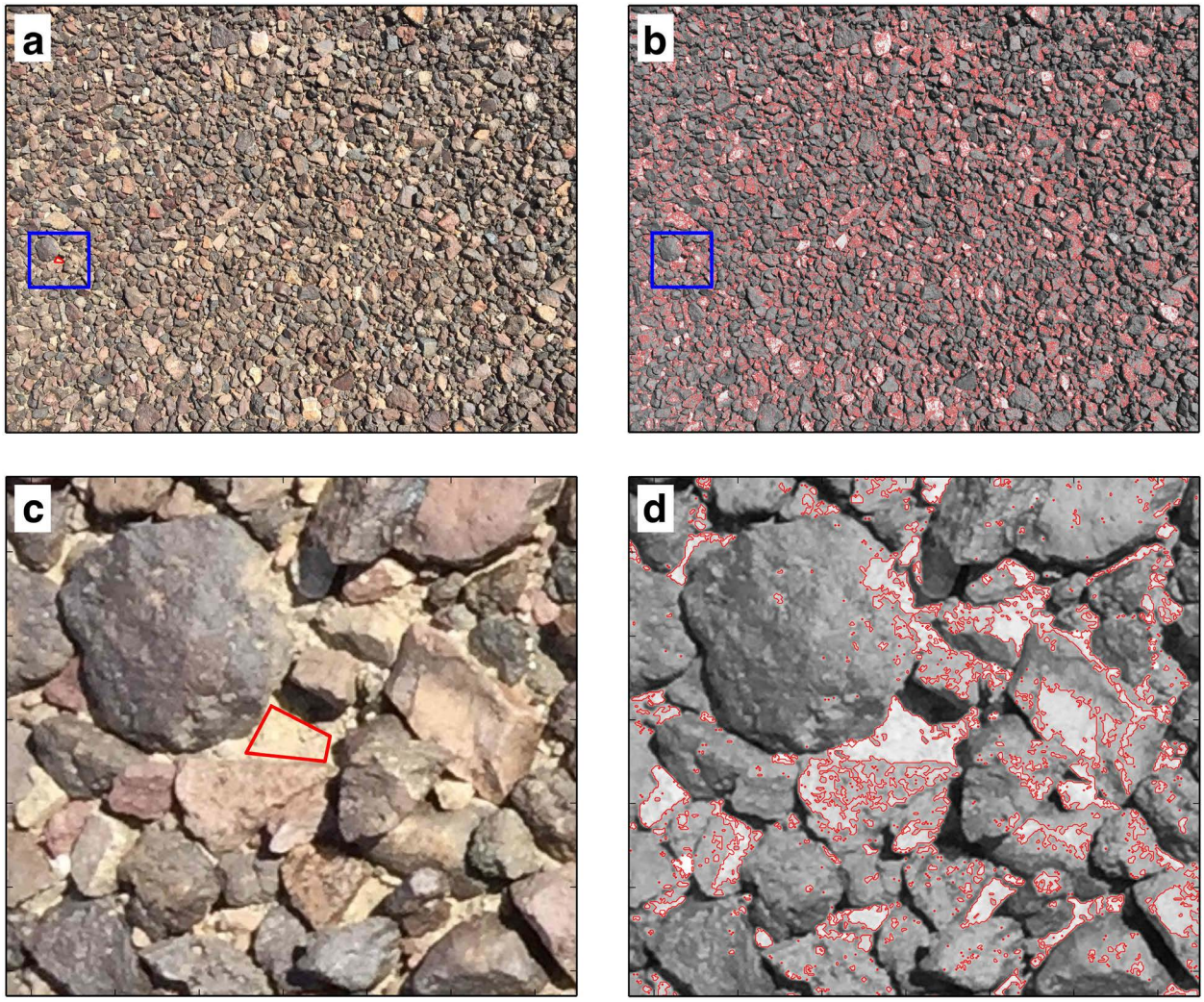

Figure S4. Estimate of pebble coverage percentage for the ALR fan surface. Mark and colors are the sample as Figure S3. Percentage of pebble coverage at this site is 87%.

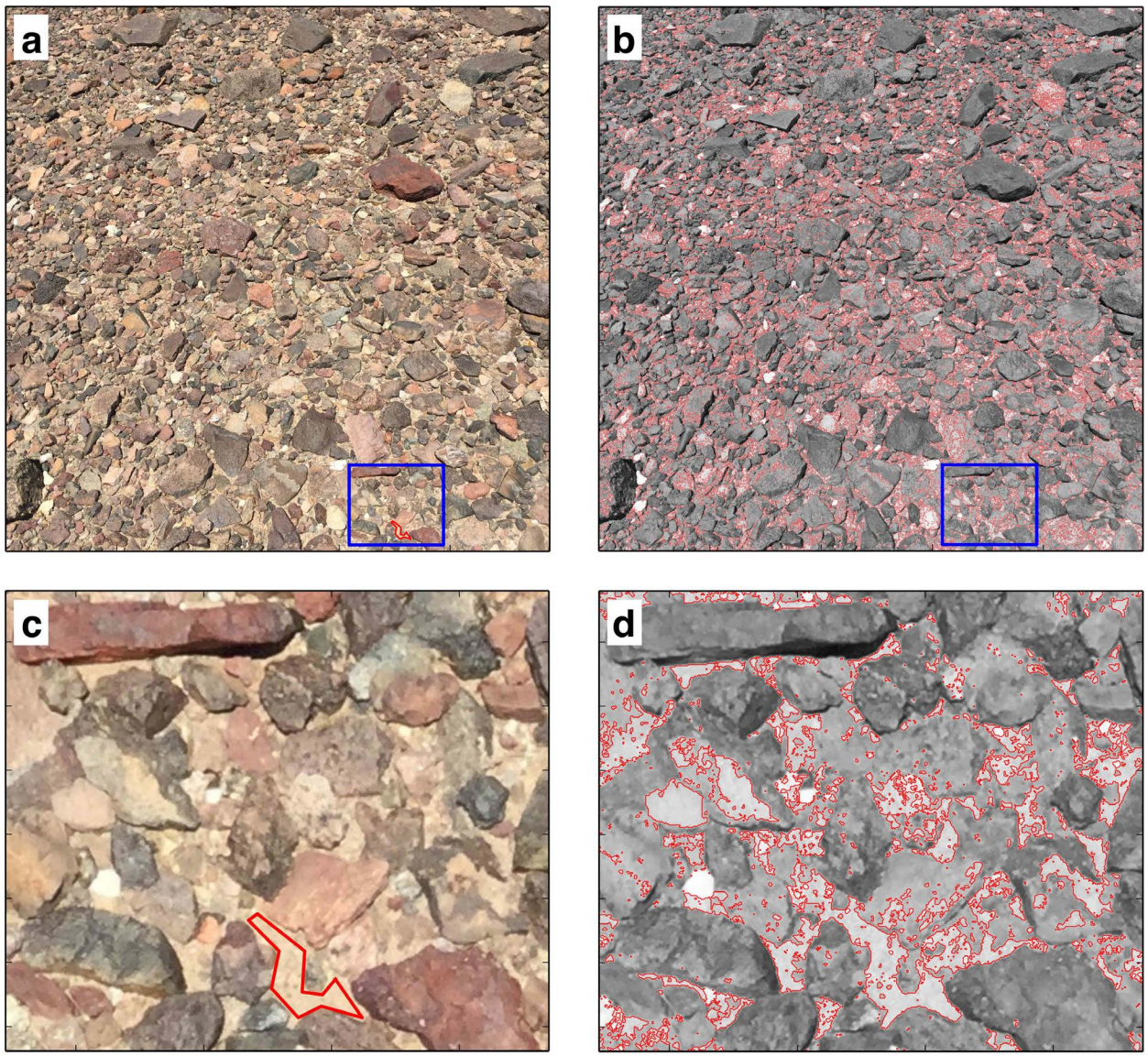

Figure S5. Estimate of pebble coverage percentage for the ALR fan surface. Mark and colors are the sample as Figure S3. Percentage of pebble coverage at this site is 87%.

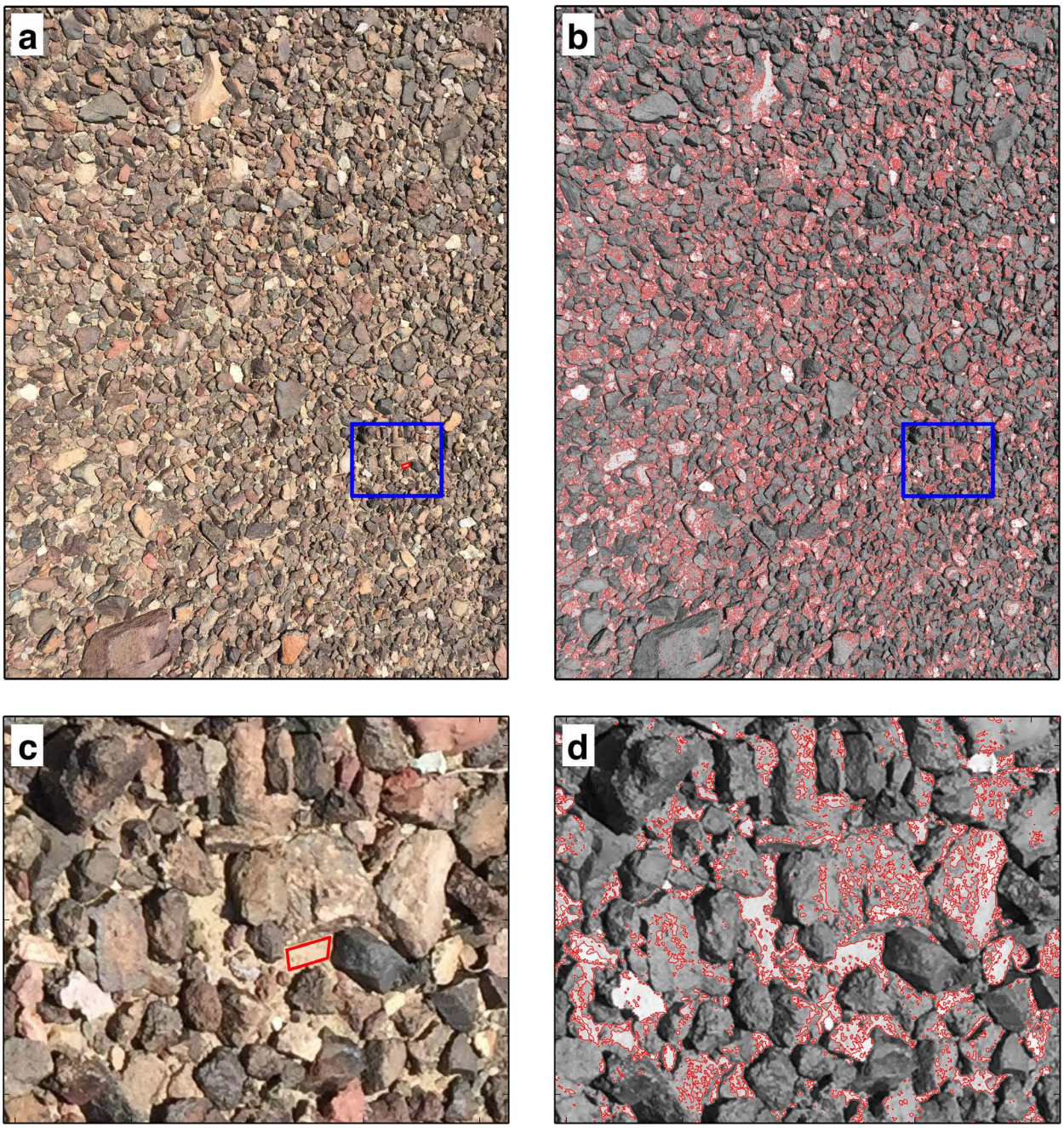

Figure S6. Estimate of pebble coverage percentage for the ALR fan surface. Mark and colors are the sample as Figure S3. Percentage of pebble coverage at this site is 86%.

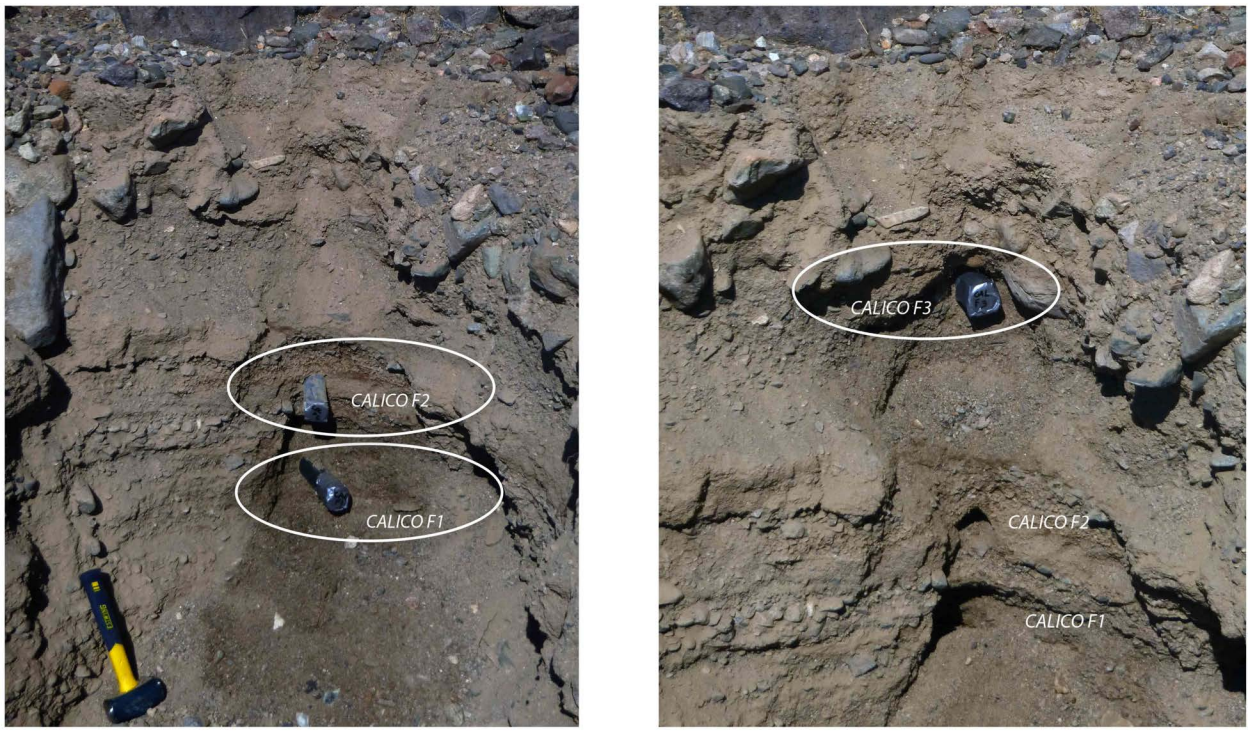

Figure S7. Samples for OSL dating. Collected at Calico-Pit2.

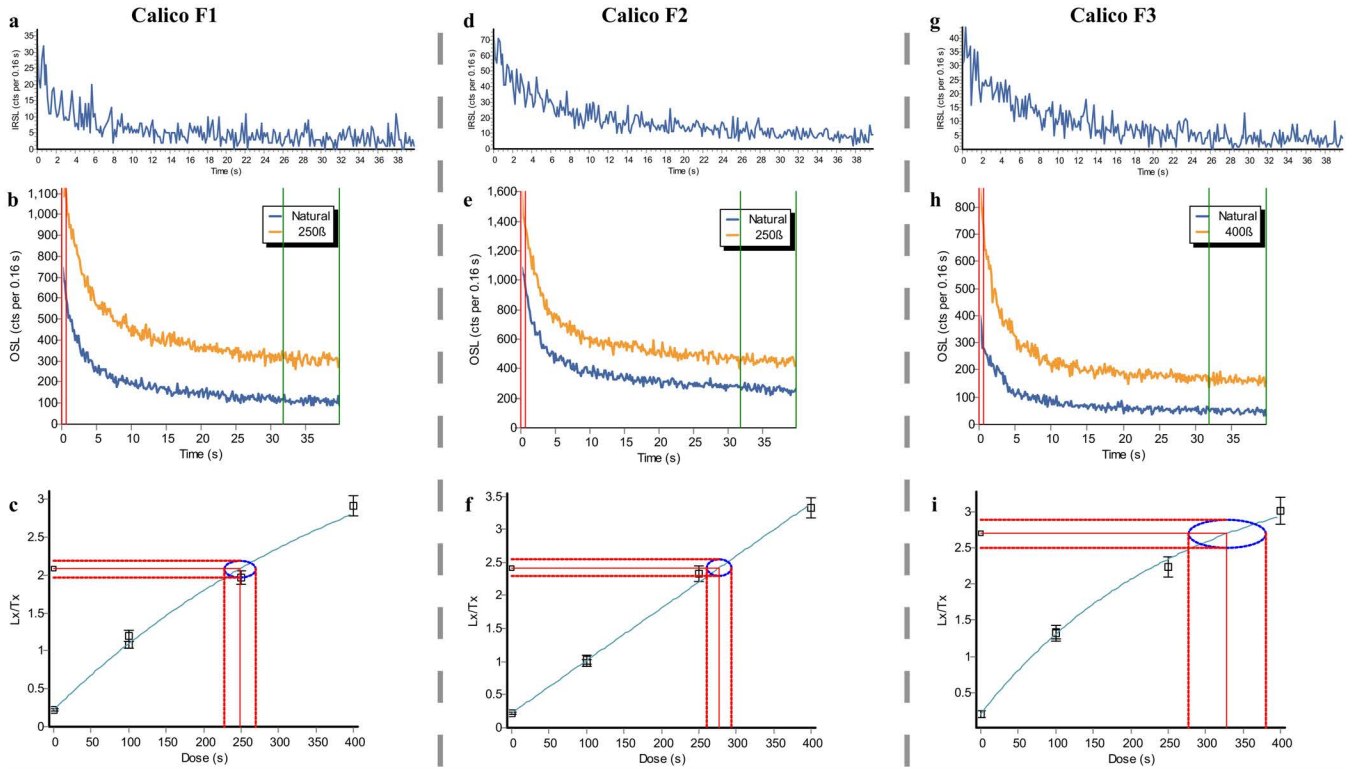

Figure S8. Examples of ISRL test for feldspar. (top) typical OSL shine down curves (middle), regenerative curves (bottom) and for each dated sample.

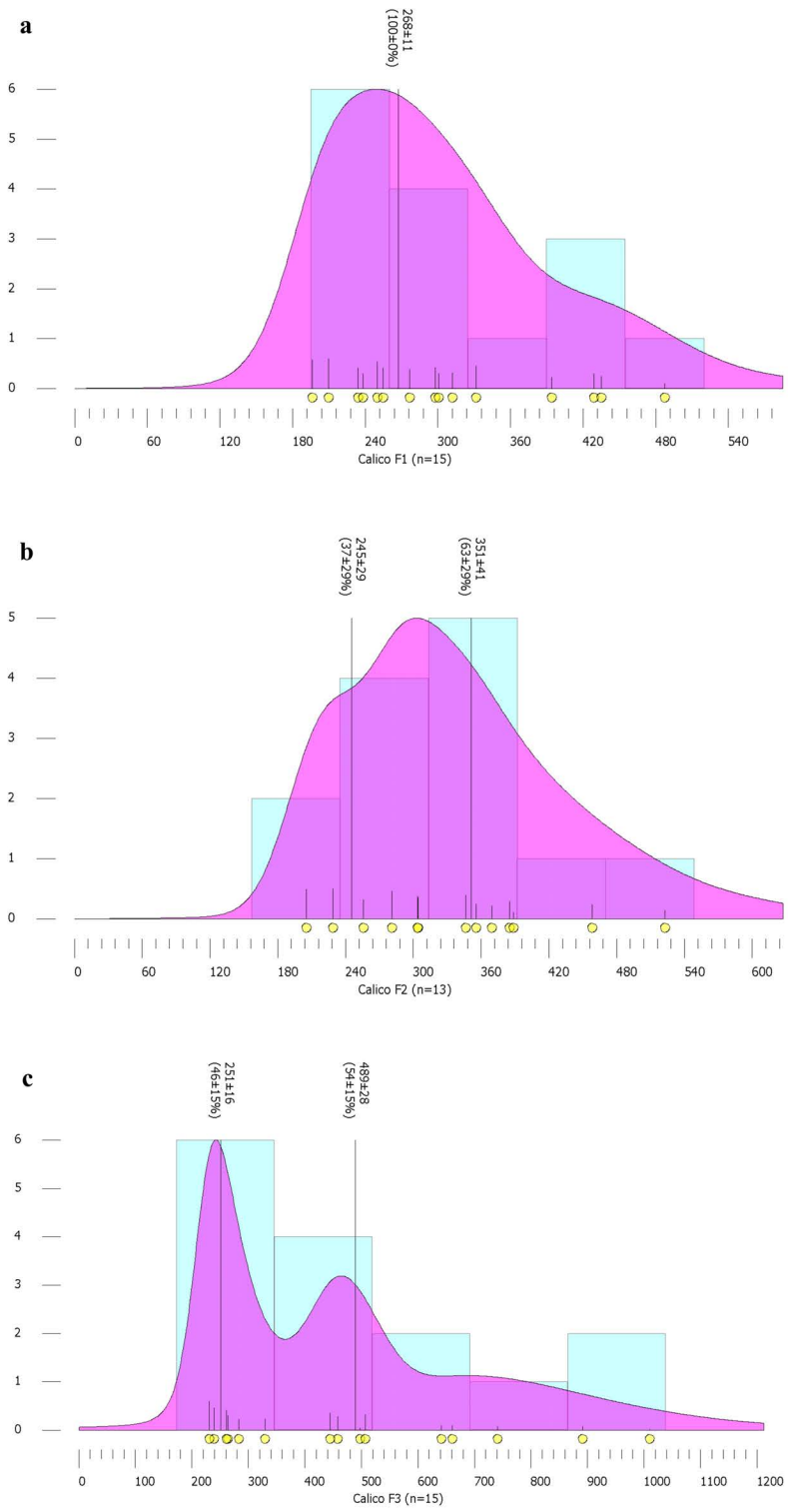

Figure S9. Equivalent doses for each sample, plotted as histograms (number of aliquots) and probability against equivalent dose (Gy).

Calico-1

Calico-2

Calico-3

Figure S10 (to be continued). Pictures of samples collected. Sample names are on the bottom-left of the corresponding pictures. Note the different level of carbonate coating for three depth profiles.

Calico-5

Calico-6

Calico-7

Figure S10 (to be continued). Pictures of samples collected. Sample names are on the bottom-left of the corresponding pictures. Note the different level of carbonate coating for three depth profiles.

Calico-8

Calico-9

Calico-11

Figure S10 (to be continued). Pictures of samples collected. Sample names are on the bottom-left of the corresponding pictures. Note the different level of carbonate coating for three depth profiles.

Calico-12

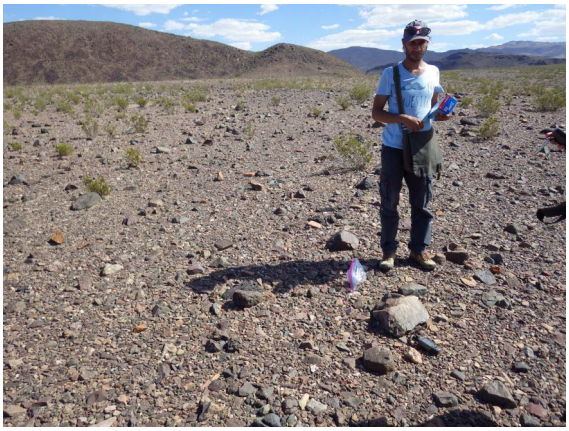

Calico-14

Calico-20

Figure S10 (to be continued). Pictures of samples collected. Sample names are on the bottom-left of the corresponding pictures. Note the different level of carbonate coating for three depth profiles.

Calico-23

Calico-25

Calico-101

Figure S10 (to be continued). Pictures of samples collected. Sample names are on the bottom-left of the corresponding pictures. Note the different level of carbonate coating for three depth profiles.

Calico-102

Calico-104

Calico-106

Figure S10 (to be continued). Pictures of samples collected. Sample names are on the bottom-left of the corresponding pictures. Note the different level of carbonate coating for three depth profiles.

Calico-107

CalicoA

Figure S10 (to be continued). Pictures of samples collected. Sample names are on the bottom-left of the corresponding pictures. Note the different level of carbonate coating for three depth profiles.

Calico-Pit2

Figure S10 (to be continued). Pictures of samples collected. Sample names are on the bottom-left of the corresponding pictures. Note the different level of carbonate coating for three depth profiles.

Calico-Pit3

Figure S10. Pictures of samples collected. Sample names are on the bottom-left of the corresponding pictures. Note the different level of carbonate coating for three depth profiles.

Table S1. Soil profile descriptions.

Profile Calico-Pit2

Horizon	Depth	Boundary	Color	Texture Class	Clay	Rock Fragment	Structure	Clay Films	Consistence		Roots	Reaction	Other Notes
	[cm]		Dry		[%]	[%]			Stickiness	Plasticity			
Avk	0-10	CS	10YR 6/4	vgr cosl	7-9	45	2m sbk	--	SO	PO	--	SL matrix	Vesicular pores
Bk1	10-30	CS	10YR 6/3	vgr cos	2-4	60	1f sbk	--	SO	PO	3f	VS matrix/ ST bottom of gravels	Stage I carbonates
Bk2	30-55	CS	7.5YR 5/3	vgr cos	0-2	50	ma	--	SO	PO	1vf	SL bottom of gravels	Stage I carbonates
2Bk	55-70	CS	7.5YR 5/3	vgr cos	0-2	60	1m sbk	--	SO	PO	1f	SL-ST masses and bottom of gravels	Stage I carbonates/transitions to stratified sands and gravels
2C	70-90	CS	10YR 5/3	vgr cos	0-2	60	ma	--	SO	PO	--	NE	Stratified sands and gravels
3BCkb	90-115		10YR 6/3	vgr s	1-3	65-70	ma	--	SO	PO	--	SL-ST matrix and filaments	Stage I carbonates/buried horizon

Profile Calico A

Horizon	Depth	Boundary	Color	Texture Class	Clay	Rock Fragment	Structure	Clay Films	Consistence		Roots	Reaction/Location	Other
	[cm]		Dry		[%]	[%]			Stickiness	Plasticity			
Desert Pavement - near complete interlocking													
Avk	0-12	CS	7.5YR 6/4	gr l	12-15	25	2f pr, 2f pl	--	SO	PO	1m, 1f	VE masses	Vesicular pores, Stage 1 carbonates
Bk1	12-28	CS	7.5 to 5YR 4/6	vgr sl	9-11	40	1f sbk	--	SO	PO	3f	VS filaments	Stage I carbonates
Bk2	28-50	CS	7.5 to 5YR 4/6	vgr cosl	7-9	60	1f sbk	--	SO	PO	3f, 1m	SL filaments	Stage I carbonates
Bk3	50-76	CS	7.5YR 4/4	vgr cosl	5-7	60	1m to f sbk	--	SO	PO	3f, 2m	ST-VE filaments and masses	Stage II carbonates
Bkk	76-142	CS	7.5YR 7/3	xgr lcos	3-5	75	ma	--	SO	PO	2f, vf	VE matrix, masses, gravels	Stage II to III carbonates
2BCk	142-152		7.5 to 5YR 4/4	gr fs	3-5	25	ma	--	SO	PO	--	SL matrix	lithologic discontinuity

Profile Calico-Pit3

Horizon	Depth	Boundary	Color	Texture Class	Clay	Rock Fragment	Structure	Clay Films	Consistence		Roots	Reaction	Other
	[cm]		Dry		[%]	[%]			Stickiness	Plasticity			
Desert Pavement - near complete interlocking													
Avk	0-10	CS	7.5YR 5/4	gr l*	18-20	30	2m sbk	--	SS	SP	1f, vf	SL masses	Vesicular pores; *bordering on sil texture
Bk1	10-35	CS	5YR 4/6	vgr l	12-15	45	2m sbk	--	SO	PO	1c, 2m, 3f	SL matrix/ST bottom of gravels	Stage I carbonates
Bk2	35-64	CS	7.5YR 6/4	xgr sl	7-9	75	ma	--	SO	PO	3f, vf	VE matrix/bottom of gravels	Stage II carbonates
BCk	64-127	CS	7.5YR 6/3	xgr cos	1-3	70	ma	--	SO	PO	--	VE matrix/bottom of gravels	Stage I-II carbonates
2BC	127-140		7.5YR 5/4	gr cos	0-2	30	ma	--	SO	PO	--	ST masses	Stage I carbonates/lithologic discontinuity

Texture Notation

Texture Class	
s	sand
sl	sandy loam
l	loam
sil	silt loam
Texture Modifier	
co	coarse
f	fine
Coarse fraction modifier	
gr	gravelly
vgr	very gravelly
xgr	extremely gravelly

Structure

Grade	
1	weak
2	moderate
Size	
f	fine
m	medium
Shape	
sbk	subangular blocky
pr	prismatic
pl	platy
ma	massive

Consistence

SO	non-sticky
SS	slightly sticky
PO	non-plastic
SP	slightly plastic

Reaction to HCl

NE	non-effervescent
VS	very slightly effervescent
SL	slightly effervescent
ST	strongly effervescent
VE	violently effervescent

Roots

Quantity	
1	few
2	common
3	many
Size	
vf	very fine
f	fine
m	medium

PDI - calculated using 4 parameters - rubification, texture, struct	
Calico-Pit2	6.0
Calico A	25.3
Calico-Pit3	18.2

References:

Harden, J.W., 1982, A quantitative index of soil development from field descriptions: Examples from a chronosequence in central California. Geoderma, v. 28(1), p.1-28. doi:10.1016/0016-7061(82)90037-4

Harden, J.W. and Taylor, E.M., 1983, A quantitative comparison of soil development in four climatic regimes. Quaternary Research, v. 20(3), p.342-359. doi:10.1016/0033-5894(83)90017-0

Table S2. Sample information and cosmogenic Be-10 analysis

Fan	Sample name	Latitude (°)	Longitude (°)	Altitude (m asl)	Sample lithology	Boulder or cobble size height/width/length (cm)	Sample thickness (cm)	Quartz msss (g)	Be carrier (g)	Be carrier concentration (mg/g)	^{10}Be / ^{9}Be [a]	Uncertainty of ^{10}Be / ^{9}Be [a]	^{10}Be concentration (atoms/g)	Uncertainty of ^{10}Be concentration (atoms/g)	Age [b] (ka)	Uncertainty of Age [b] (ka)
ALR	Calico-9 [a1]	34.80653	-116.63991	565	Quartz cobble	6×13×14	6	26.3343	0.3511	1.0255	1.9901E-12	3.0061E-14	1.8182E+06	2.7465E+04	345.71	12.14
ALR	Calico-11 [a1]	34.80516	-116.64095	574	Quartz cobble	10×14×16	10	22.1755	0.3497	1.0255	1.5014E-12	2.1331E-14	1.6225E+06	2.3051E+04	313.67	10.22
ALR	Calico-12 [a1]	34.80386	-116.64128	574	Quartz cobble	9×11×13	9	23.0785	0.3490	1.0255	3.9628E-13	1.8108E-14	4.1066E+05	1.8765E+04	75.28	4.17
ALR	Calico-14 [a3]	34.80536	-116.63969	574	Quartz cobble	6×7×10	6	27.1480	0.3489	1.0038	7.6109E-13	1.5613E-14	6.5610E+05	1.3459E+04	113.56	3.78
ALR	Calico-20 [a1]	34.80507	-116.63848	582	Rhyolite boulder	25×55×90	5	29.6960	0.3509	1.0255	7.8789E-13	9.2888E-14	6.3799E+05	7.5216E+04	112.13	12.69
ALR	Calico-23 [a1]	34.80766	-116.64798	563	Granitic boulder	15×30×30	5	13.0553	0.3492	1.0255	2.4767E-13	3.4168E-14	4.5396E+05	6.2629E+04	81.48	11.60
ALR	Calico-25 [a1]	34.80818	-116.65013	565	Granite boulder	20×40×40	3	3.2115	0.3496	1.0255	1.2513E-13	4.3672E-15	9.3319E+05	3.2569E+04	106.99	9.76
ALR	CA-104 [a3]	34.80656	-116.64688	574	Vein quartz boulder	15×30×30	4	19.7600	0.3508	1.0038	4.7687E-13	1.2370E-14	5.6787E+05	1.4730E+04	100.20	3.61
ALR	CA-106 [a3]	34.80446	-116.64082	581	Gneiss boulder	25×40×50	4	5.0778	0.3507	1.0038	1.0178E-13	7.4584E-15	4.7150E+05	3.4553E+04	82.80	6.65
ALR	CA-107 [a3]	34.80477	-116.64095	579	Quartz cobble	8×10×13	3	17.2178	0.3496	1.0038	4.0526E-13	1.2214E-14	5.5196E+05	1.6635E+04	96.48	3.77
ALR	CalicoA-25 [a2]	34.80141	-116.64094	597	Sand	NA	5	3.2115	0.3495	1.0255	1.2513E-13	4.3672E-15	9.3319E+05	3.2569E+04	NA	NA
ALR	CalicoA-50 [a2]	34.80141	-116.64094	597	Sand	NA	5	7.1261	0.3491	1.0255	1.1622E-13	2.8466E-15	3.9016E+05	9.5562E+03	NA	NA
ALR	CalicoA-75 [a2]	34.80141	-116.64094	597	Sand	NA	5	9.6515	0.3487	1.0255	1.5594E-13	4.9884E-15	3.8608E+05	1.2351E+04	NA	NA
ALR	CalicoA-140 [a2]	34.80141	-116.64094	597	Sand	NA	5	12.4054	0.3492	1.0255	1.1463E-13	7.2138E-15	2.2112E+05	1.3915E+04	NA	NA
ALR	Calico-Pit3-30 [a4]	34.80666	-116.64672	574	Sand	NA	5	5.2169	0.3513	1.0038	9.3243E-14	6.8176E-15	4.2117E+05	3.0795E+04	NA	NA
ALR	Calico-Pit3-55 [a4]	34.80666	-116.64672	574	Sand	NA	5	9.3469	0.3486	1.0038	1.7439E-13	4.8891E-15	4.3627E+05	1.2231E+04	NA	NA
ALR	Calico-Pit3-80 [a4]	34.80666	-116.64672	574	Sand	NA	5	7.1150	0.3493	1.0038	1.1448E-13	4.0200E-15	3.7698E+05	1.3238E+04	NA	NA
ALR	Calico-Pit3-110 [a4]	34.80666	-116.64672	574	Sand	NA	5	9.1696	0.3484	1.0038	1.2712E-13	4.0966E-15	3.2399E+05	1.0441E+04	NA	NA
ALR	Calico-Pit3-145 [a4]	34.80666	-116.64672	574	Sand	NA	5	12.2961	0.3499	1.0038	1.5653E-13	4.4406E-15	2.9877E+05	8.4762E+03	NA	NA
ALR	Calico-Pit3-180 [a4]	34.80666	-116.64672	574	Sand	NA	5	5.8953	0.3506	1.0038	7.1740E-14	4.4839E-15	2.8618E+05	1.7887E+04	NA	NA
TR	Calico-1 [a1]	34.79170	-116.63715	605	Granite boulder	25×30×45	2.5	7.6464	0.3513	1.0255	3.1442E-14	2.1093E-15	9.8992E+04	6.6409E+03	17.13	1.15
TR	Calico-2 [a1]	34.79123	-116.63741	608	Granite boulder	25×25×45	3	5.9949	0.3490	1.0255	1.7044E-14	1.5816E-15	6.7994E+04	6.3097E+03	12.09	1.10
TR	Calico-3 [a1]	34.79081	-116.63744	608	Granite boulder	25×30×55	4	11.9578	0.3499	1.0255	1.2301E-13	4.4861E-15	2.4666E+05	8.9955E+03	41.42	1.65
TR	Calico-5 [a1]	34.79073	-116.63713	610	Granite boulder	15×15×30	5	29.9644	0.3494	1.0255	1.1230E-13	1.4790E-14	8.9738E+04	1.1818E+04	15.90	1.94
TR	Calico-6 [a1]	34.80653	-116.63991	565	Granite boulder	40×60×65	4	14.5044	0.3500	1.0255	8.5267E-13	3.3342E-14	1.4100E+06	5.5135E+04	249.74	12.46
TR	Calico-7 [a1]	34.80516	-116.64095	574	Granite boulder	15×30×50	4	8.9600	0.3494	1.0255	9.5295E-14	9.1324E-15	2.5465E+05	2.4404E+04	42.51	3.91
TR	Calico-8 [a1]	34.80386	-116.64128	574	Granite boulder	15×50×85	4	14.1046	0.3504	1.0255	2.0565E-13	7.0207E-15	3.5010E+05	1.1952E+04	59.63	2.53
TR	CA-101 [a3]	34.80536	-116.63969	597	Granodiorite boulder	40×45×65	4	8.0275	0.3489	1.0038	2.0478E-14	2.7547E-15	5.9701E+04	8.0311E+03	10.90	1.37
TR	CA-102 [a3]	34.79148	-116.63808	599	Granodiorite boulder	25×30×60	3	9.3056	0.3515	1.0038	1.6235E-13	1.0499E-14	4.1135E+05	2.6602E+04	69.89	4.95
TR	Calico-Pit2-20 [a2]	34.79250	-116.63712	596	Sand	NA	5	23.2012	0.3488	1.0038	3.3138E-13	7.4765E-15	3.3417E+05	7.5395E+03	NaN	NA
TR	Calico-Pit2-35 [a2]	34.79250	-116.63712	596	Sand	NA	5	19.9183	0.3523	1.0038	2.7070E-13	5.7384E-15	3.2116E+05	6.8081E+03	NaN	NA
TR	Calico-Pit2-70 [a2]	34.79250	-116.63712	596	Sand	NA	5	21.7258	0.3493	1.0038	3.0524E-13	6.7068E-15	3.2919E+05	7.2329E+03	NaN	NA
TR	Calico-Pit2-105 [a2]	34.79250	-116.63712	596	Sand	NA	5	11.4099	0.3503	1.0038	1.5749E-13	4.7380E-15	3.2434E+05	9.7573E+03	NaN	NA
TR	Calico-Pit2-130 [a2]	34.79250	-116.63712	596	Sand	NA	5	16.9731	0.3480	1.0038	2.4156E-13	6.0297E-15	3.3221E+05	8.2925E+03	NaN	NA
TR	Calico-Pit2-165 [a2]	34.79250	-116.63712	596	Sand	NA	5	17.1076	0.3485	1.0038	2.4397E-13	5.6989E-15	3.3337E+05	7.7872E+03	NaN	NA
TR	Calico-Pit2-190 [a2]	34.79250	-116.63712	596	Sand	NA	5	16.4650	0.3486	1.0038	2.3385E-13	5.7084E-15	3.3210E+05	8.1070E+03	NaN	NA

a. Background corrected by blanks run concurrents with sample measurements. ^{10}Be / ^{9}Be and ^{10}Be concentration uncertainties are reported with 65% confidence interval (1-sigma). Blank ^{10}Be / ^{9}Be values used to correct for backgrounds are: a1, $1.14\pm0.64\times10^{-15}$; a2, $1.63\pm0.36\times10^{-15}$; a3, $2.32\pm0.59\times10^{-15}$; a4, $0.82\pm0.33\times10^{-15}$.

b. Use reference production rate of 4.21±0.13 atoms/g/yr for the Western USA and scaled to latitude and pressure at the sample locations [Nishiizumi et al., 1989; Lal, 1991; Stone, 2000; Balco et al., 2008]. Atmosphere Model is ERA40 [Uppala et al., 2005]. Geomagnetic database from Muscheler et al. [2005] and Valet et al. [2005]. Ages are calculated with online Cosmic Ray Exposure program (CREp: crep.crpg.cnrs-nancy.fr) [Martin et al., 2017]. Age errors are reported with 65% confidence interval (1-sigma). Different scaling models produce age difference not significant enough (<15%) to alter our interpretations.